Evolutionary plasticity of SH3 domain binding by Nef proteins of the HIV-1/SIVcpz lentiviral lineage

Zhe Zhao[1], Riku Fagerlund[1], Daniel Sauter[2,3], Helena Tossavainen[4], Perttu Permi[4,5], Frank Kirchhoff[2] and Kalle Saksela[1*]

[1] Department of Virology, University of Helsinki and Helsinki University Hospital, Helsinki, Finland

[2] Institute of Molecular Virology, Ulm University Medical Center, 89081 Ulm, Germany.

[3] Institute for Medical Virology and Epidemiology of Viral Diseases, University Hospital Tübingen, 72076 Tübingen, Germany.

[4]Department of Biological and Environmental Science, University of Jyväskylä, Jyväskylä, Finland

[5]Department of Chemistry, Nanoscience Center, University of Jyväskylä, Jyväskylä, Finland.

Short title: Evolving SH3 binding strategies of lentiviral Nef proteins

*Correspondence:
Kalle Saksela
Department of Virology, University of Helsinki
PO Box 21 (Haartmaninkatu 3), 00014-University of Helsinki, Finland
Tel: +358 2 9412 6770
Fax: +358 2 9412 6491
E-mail: kalle.saksela@helsinki.fi

ABSTRACT

The accessory protein Nef of human and simian immunodeficiency viruses (HIV and SIV) is an important pathogenicity factor known to interact with cellular protein kinases and other signaling proteins. A canonical SH3 domain binding motif in Nef is required for most of these interactions. For example, HIV-1 Nef activates the tyrosine kinase Hck by tightly binding to its SH3 domain. An archetypal contact between a negatively charged SH3 residue and a highly conserved arginine in Nef (Arg77) plays a key role here. Combining structural analyses with functional assays, we here show that Nef proteins have also developed a distinct structural strategy - termed the "R-clamp" - that favors the formation of this salt bridge via buttressing Arg77. Comparison of evolutionarily diverse Nef proteins revealed that several distinct R-clamps have evolved that are functionally equivalent but differ in the side chain compositions of Nef residues 83 and 120. Whereas a similar R-clamp design is shared by Nef proteins of HIV-1 groups M, O, and P, as well as SIVgor, the Nef proteins of SIV from the Eastern chimpanzee subspecies (SIVcpz$^{P.t.s.}$) exclusively utilize another type of R-clamp. By contrast, SIV of Central chimpanzees (SIVcpz$^{P.t.t.}$) and HIV-1 group N strains show more heterogenous R-clamp design principles, including a non-functional evolutionary intermediate of the aforementioned two classes. These data add to our understanding of the structural basis of SH3 binding and kinase deregulation by Nef, and provide an interesting example of primate lentiviral protein evolution.

AUTHOR SUMMARY

Viral replication depends on interactions with a plethora of host cell proteins. Cellular protein interactions are typically mediated by specialized binding modules, such as the SH3 domain. To gain access to host cell regulation viruses have evolved to contain SH3 domain binding sites in their proteins, a notable example of which is the HIV-1 Nef protein. Here we show that during the primate lentivirus evolution the structural strategy that underlies the avid binding of Nef to cellular SH3 domains, which we have dubbed the R-clamp, has been generated via alternative but functionally interchangeable molecular designs. These patterns of SH3 recognition depend on the amino acid combinations at the positions corresponding to residues 83 and 120 in the consensus HIV-1 Nef sequence, and are distinctly different in Nef proteins from SIVs of Eastern and Central chimpanzees, gorillas, and the four groups of HIV-1 that have independently originated from the latter two. These results highlight the evolutionary plasticity of viral proteins, and have implications on therapeutic development aiming to interfere with SH3 binding of Nef.

INTRODUCTION

Primate lentiviruses comprise human immunodeficiency viruses (HIV-1 and HIV-2), as well as more than 40 simian immunodeficiency viruses (SIVs) infecting non-human primate species from sub-Saharan Africa. HIV-1 groups M, N, O, and P originate from four independent transmissions of SIV from Central chimpanzees (SIVcpz$^{P.t.t.}$) and gorillas (SIVgor) to humans, whereas HIV-2 groups A to I are derived from nine zoonotic transmissions of SIV from sooty mangabeys (SIVsmm) (reviewed in [1]). SIVsmm was also transmitted to macaques, giving rise to SIVmac. The global AIDS pandemic is largely caused by HIV-1 group M strains, which are further divided into 10 subtypes (A, B, C, D, F, G, H, J K, and L), as well as several sub-subtypes and circulating recombinant forms [2-4].

The viral protein Nef is a multifunctional accessory factor encoded by all primate lentiviruses. While *nef*-defective HIV and SIV are replication-competent, infections with such viruses are associated with low viral loads and no or delayed pathogenesis in humans or experimentally infected macaques [5]. Nef itself exhibits no enzymatic activity but instead modulates host cell function by interacting with a plethora of other proteins to hijack cellular signaling and membrane trafficking pathways [6-8].

A function of HIV-1 Nef that is well understood at the molecular and mechanistic level is its interaction with Hck, a member of the Src-family tyrosine kinases. Nef tightly binds to the SH3 domain of Hck, thereby pushing it from an intramolecular autoinhibitory state into a catalytically active conformation [9, 10]. Hck plays an important role in regulating activation and effector functions of macrophages, the second main target cell population of HIV-1 besides $CD4^+$ T cells [11, 12]. Many Nef functions in other cell types including T lymphocytes, (e.g., MHC-I downregulation [13], interfering with Lck localization and immunological synapse formation [13], and reorganization of the actin cytoskeleton [14, 15]) are also strictly

dependent on its SH3 binding capacity. However, the relevant SH3 proteins in these cells do not bind to Nef as tightly as Hck, and have therefore remained less well characterized [7].

The discovery of the Nef-Hck interaction provided the first example of pathogen takeover of host cell signaling via SH3 domain ligand mimicry [16]. Src Homology 3 (SH3) domains are short (~60 aa) modular protein units specialized for mediating protein interactions via proline-rich core binding sites in the target proteins, and are ubiquitous (~300 in human) in eukaryotic proteins involved in regulation of cell behavior [17, 18].

Studies on the Nef-SH3 complex also revealed a new paradigm for the structural basis of SH3 binding: It could be shown that docking of the proline-rich (PxxP) peptide of Nef by the SH3 core binding interface is assisted by further molecular contacts of the so-called SH3 RT-loop region to provide additional specificity and affinity to this interaction [9]. The amino acid residues that form a binding pocket for the RT-loop of the Hck-SH3 domain are highly conserved in HIV-1 and HIV-1-like Nef proteins, and provide them with a capacity for strong binding to Hck [9, 19]. Nef proteins from the HIV-2/SIVsmm groups lack these residues and hence Hck binding capacity, but as evidenced by the SIVmac293-Y113W/E117T/E118Q triple mutant [20], can acquire this function upon introduction of just a few key residues from HIV-1 Nef.

We have recently shown that Hck activation by Nef leads to Raf/MAPK pathway activation and triggers the secretion of proinflammatory cytokines [19, 21]. In agreement with their enhanced affinity for Hck [9, 20], we found that only HIV-1/SIVcpz type Nef proteins but not HIV-2/SIVsmm type Nef proteins show this function. The current study was incited by our observation that an HIV-1 group N Nef (clone YBF30) was unable to bind and activate Hck and the Raf/MAPK pathway for reasons that could not be readily explained by its amino acid sequence. Our investigation into this issue led to the discovery of a structural arrangement that we have termed the arginine R-clamp and characterized here. We show

that different but functionally equivalent R-clamps have emerged in the HIV-1/SIVcpz lineage to coordinate Hck SH3 domain binding by Nef. This finding further highlights the importance of Nef-mediated SH3 binding and the enormous plasticity of primate lentiviral accessory proteins.

RESULTS

In our previous studies we examined the capacity of Nef to activate Hck by monitoring tyrosine phosphorylation of paxillin, a prominent substrate for Src family tyrosine kinases, and by measuring the induction of AP-1-regulated reporter gene expression following Hck-activated MAPK signaling [19, 21]. When additional Nef proteins from HIV-1 groups N, O, and P were examined (Figure 1), we unexpectedly noticed that the Nef protein of HIV-1 N YBF30 (AJ006022) was unable to induce paxillin phosphorylation or AP-1 activity despite sharing the ^{72}PxxPxR^{77} motif (numbering based on the HIV-1 Nef consensus) known to be important for Hck binding by HIV-1/SIVcpz type Nefs (Figure 2). Importantly, YBF30 Nef was expressed well in these cells (Figure 1A), and as also shown previously [22] was fully functional when tested for its capacity to downregulate cell surface expression of CD4 (Figure 1C and Supplementary Figure 1).

To examine if this is a characteristic of several HIV-1 group N viruses we tested three additional HIV-1 N Nef proteins from the strains 02CM-DJO0131 (AY532635), YBF106 (AJ271370), and S4858 (KY498771). However, we found that all of them were fully competent for Hck activation, and induced paxillin phosphorylation and AP-1 activity as efficiently as Nef from the widely used HIV-1 group M strain SF2 (Figure 1).

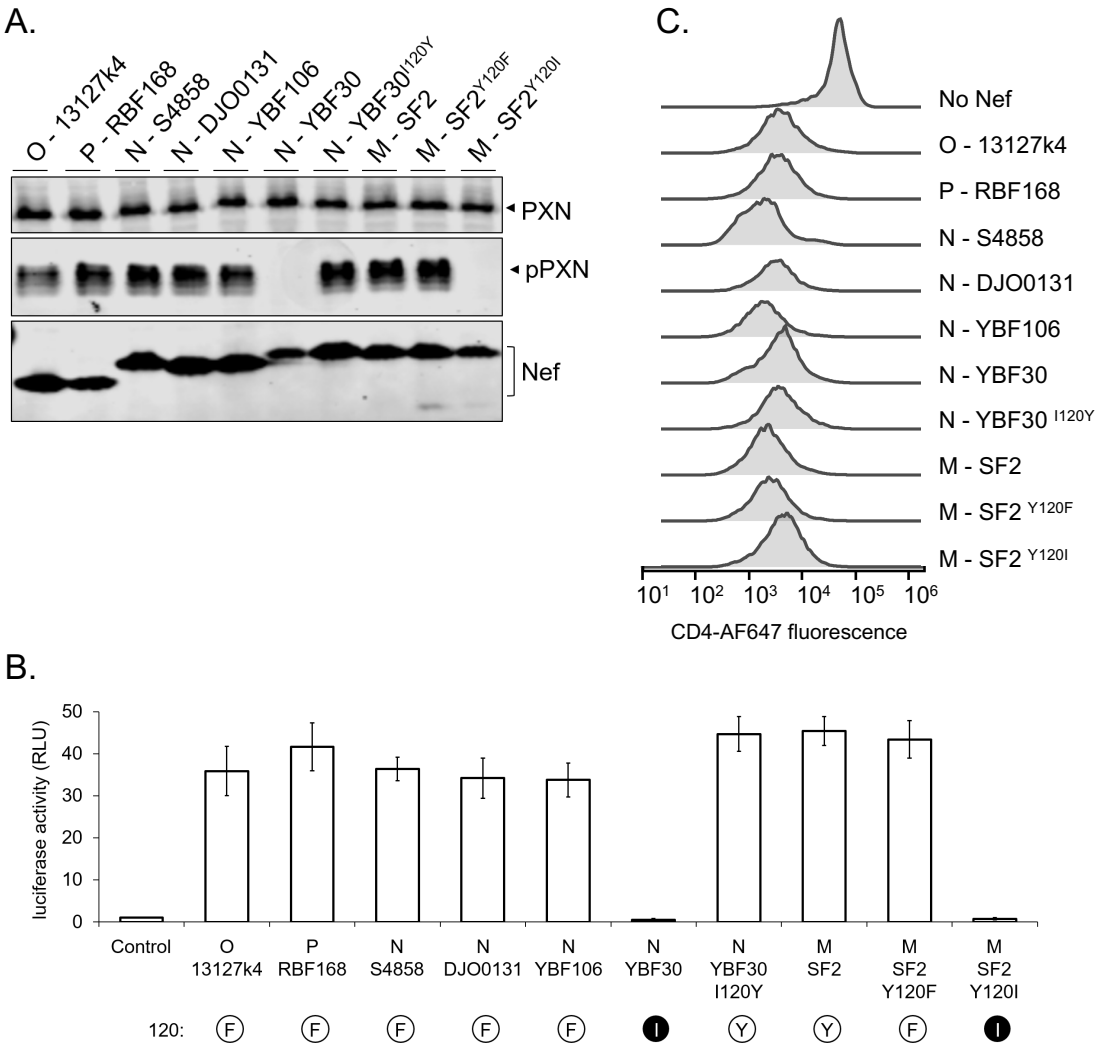

FIGURE 1. Hck-activating potential of selected HIV-1 Nefs. (A) Hck-expressing HZ-1 cells were co-transfected with vectors for paxillin and Nef from the indicated HIV-1 group M, N, O or P clones, or mutants thereof. Lysates of the transfected cells were analyzed by Western blotting using antibodies against paxillin (PXN), phosphorylated paxillin (pPXN) and Nef. **(B)** HZ-1 cells were transfected with an AP-1 transcription factor-driven luciferase reporter alone (Control) or together with the indicated Nefs variants. Luciferase activity was measured in cells harvested 24 h post-transfection, and normalized to the corresponding control sample that was set to 1. The data shown are derived from three independent experiments, with SE indicated by error bars. The amino acid at position 120 of each Nef protein is indicated, aromatic residues are shown as a black 1-letter symbol in a white sphere, and isoleucine as a white letter in a black sphere. **(C)** Jurkat T cells stably expressing CD4 were infected with lentiviral vectors expressing GFP alone (No Nef) or together with plasmids expressing the indicated Nefs. CD4 down-regulation by Nef was measured using flow cytometry 48 h after

lentiviral transduction, and histograms illustrating cell surface levels of CD4 among the GFP positive Jurkat cells are shown. Original dot plots are shown in Fig. S1.

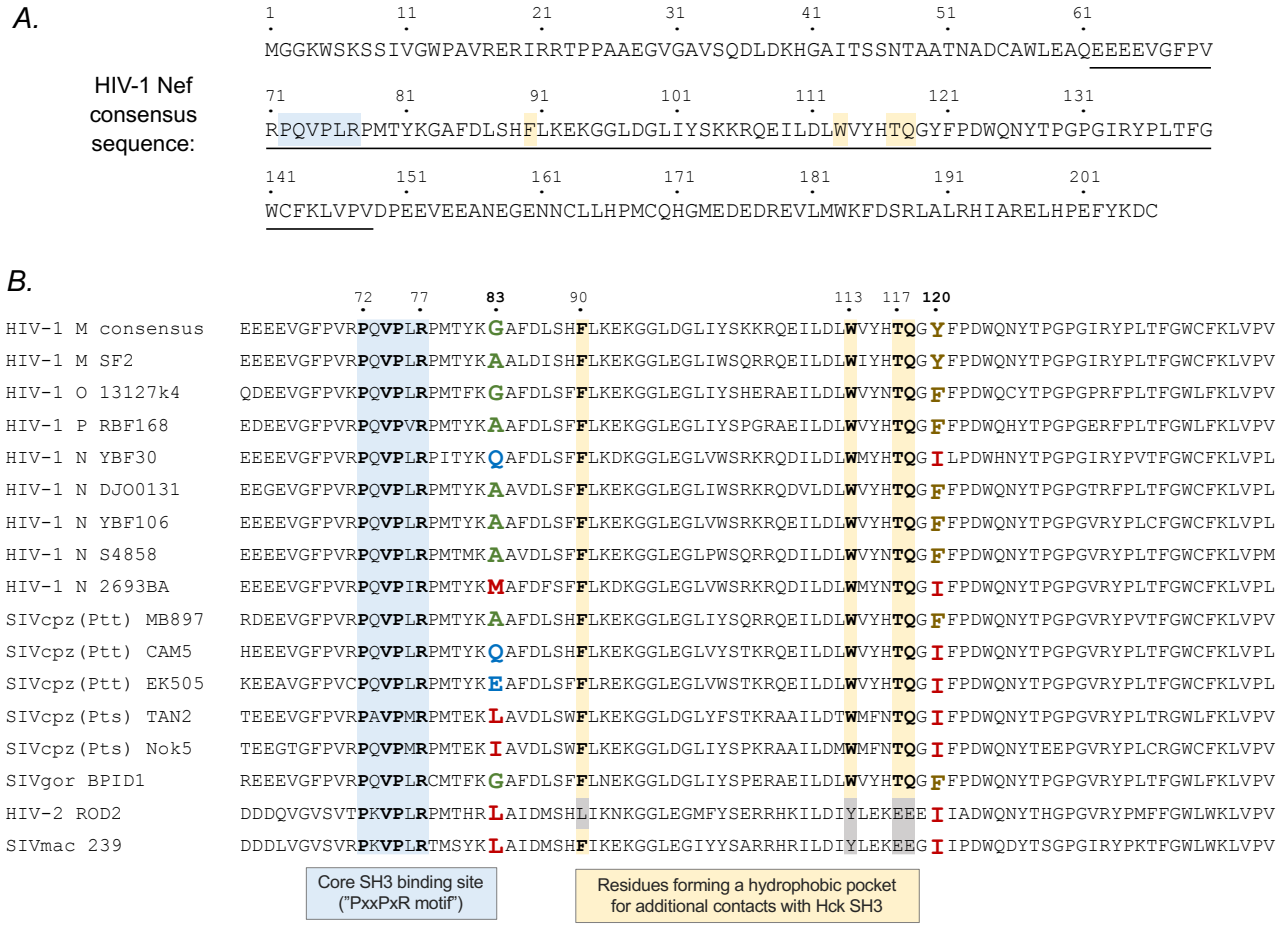

FIGURE 2: HIV-1 M consensus Nef amino acid sequence **(A)** and an alignment of the conserved central region (underlined in A) of selected Nef proteins from different primate lentiviruses **(B)**. The key residues of the core SH3 docking site (PxxPxR motif), including Arg77, are highlighted in light blue. Residues involved in a binding pocket for the Hck SH3 domain RT-loop that are conserved in HIV-1 and HIV-1-like Nef proteins are highlighted in yellow. Residues at positions 83 and 120 forming the R-clamp coordinating the positioning of Arg77 are shown in bold and colored according to their side chain properties (small in green, hydrophilic in blue, aliphatic or methionine in red, aromatic in brown). The names of HIV/SIV strains from which Nef proteins were included in this study are shown on the left.

Since the core SH3 docking motif (^{72}PxxPxR^{77}) as well as the key RT-loop accommodating residues, including Phe90, Trp113, Thr117, and Gln118, were conserved in YBF30 Nef (see Figure 2) we had a more detailed look at the original X-ray structure of the HIV-1 Nef-SH3 complex (1EFN; [9]), which directed our attention to Nef residue 120. This position is occupied by an aromatic residue (tyrosine or phenylalanine) in virtually all HIV-1 M Nef proteins, while an isoleucine residue is found in this position in YBF30 Nef (Figure 2).

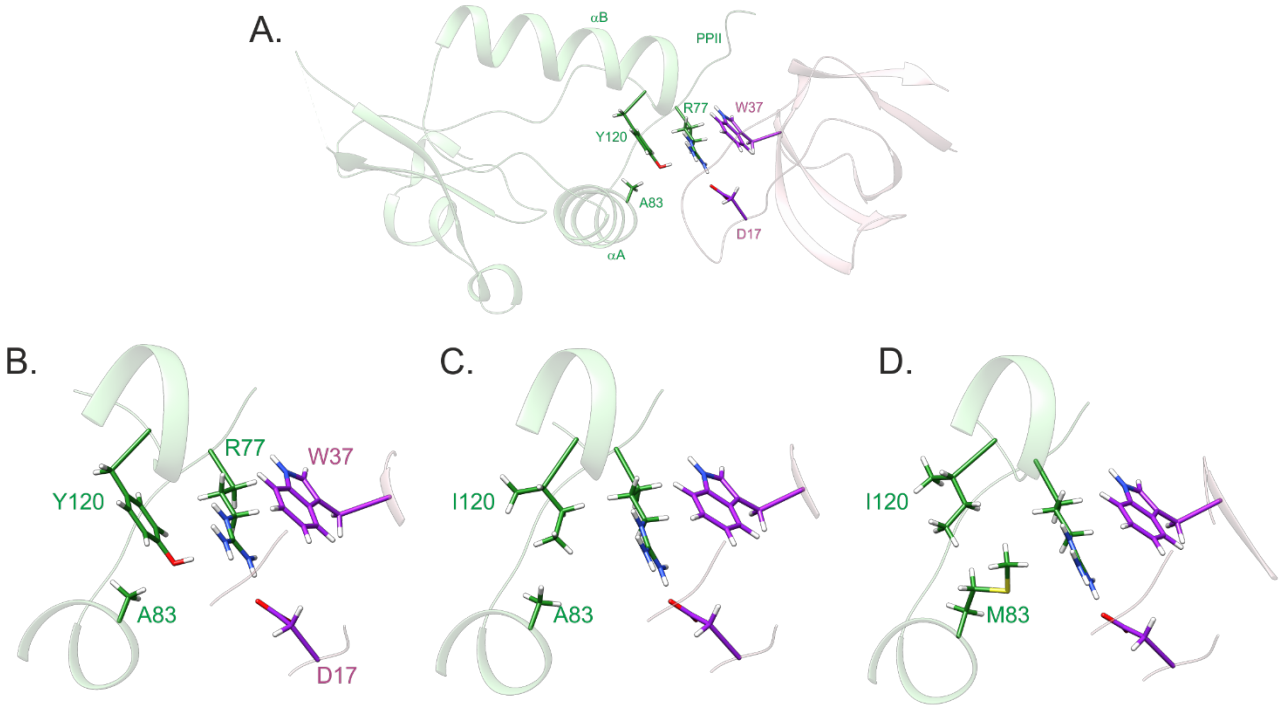

FIGURE 3: The arginine clamp. (A) Structure of the HIV-1 Nef (green) – SH3 (pink) complex (PDB ID 1EFN) highlighting critical residues in the interaction interface. **(B)** Close up view of the R clamp, stabilized by stacked Y-R-W side chains and a salt bridge between R77 (Nef) and D17 (SH3) side chains. **(C)** In the Y120I structure, one side of the R77 guanidinium plane is lacking non-bonded interactions. **(D)** In the A83M/Y120I, structure the long methionine side chain re-establishes non-bonded contacts for R77. The presented mutated complex structures were created by replacing Y120 or Y120 and A83 in UCSF Chimera [23] and minimizing the structures with AMBER [24].

In the 1EFN structure, Y120 can be seen to coordinate the Nef-SH3 interaction by buttressing the side-chain of the R77 in the Nef ^{72}PxxPxR^{77} motif together with the SH3 residue W37 (SH3 numbering according to [18]) in order to stabilize the close positioning of R77 with the acidic SH3 residue D17 to form a critical salt bridge with it (Figure 3A and B). We termed this steric guiding of the Nef residue R77 into close proximity of D17 in Hck-SH3 the "arginine (R)-clamp", and hypothesized that the failure of YBF30 Nef to activate Hck is due to the failure of its Ile120 residue to from a functional R-clamp (Figure 3C).

In support of this hypothesis, we found that YBF30 Nef became fully competent for Hck activation when its Ile120 residue was replaced by a tyrosine (YBF30 I120Y) (Figure 1). We then further investigated this idea by changing the Y120 residue in the Nef protein from the HIV-1 M laboratory strain SF2 into an YBF30-like isoleucine (Nef mutant SF2 Y120I) or into a phenylalanine, the other commonly found residue at this position (Nef mutant SF2 Y120F). While the conservative Y120F amino acid change did not affect Hck activation, the Y120I mutation recapitulated the failure of YBF30 Nef to stimulate paxillin phosphorylation and AP-1 activity, without compromising protein stability or CD4 downregulation (Figure 1). Thus, we conclude that the lack of a functional R-clamp due to the I120 residue likely explains the inability of YBF30 Nef to activate Hck.

Analysis of additional HIV-1 group N Nefs revealed that in 5 out of the total of 12 sequences that are available in databases the position 120 was occupied by Ile (Table 1). This is in stark contrast to the Nef proteins from the three other HIV-1 groups M, O, and P, in which residue 120 is invariably Tyr or Phe. We had access to another Ile120-containing HIV-1 N Nef namely 2693BA (GQ925928), and went on to examine its ability to activate Hck. Having already established a strict correlation between paxillin phosphorylation and AP-1 activity as markers of Hck activation (Fig. 1 and Zhao et al 2021), we chose to focus on using AP-1-driven reporter gene expression as the read-out in our further studies. Unexpectedly, we found that despite

carrying the I120 residue 2693BA Nef had an undiminished capacity to activate Hck (Figure 4). In order to understand this finding, we returned to the Nef-SH3 structure 1EFN, and noted the involvement of Nef residue 83 in contacting the critical R-clamp residue 120 (Figure 3). Residue 83 is an amino acid with a tiny (Ala or Gly) or a hydrophilic side-chain (Gln, Ser, Asp, or Glu) in virtually all Nef proteins that have an aromatic (Phe or Tyr) residue at position 120. However, in 2693BA Nef position 83 is occupied by methionine, a residue with a large hydrophobic/aliphatic side-chain. We therefore hypothesized that M83 might compensate for the presence of isoleucine instead of a planar aromatic residue at position 120 (Figure 3D and Supplementary Figure 4), and that the M83/I120 residue pair of 2693BA Nef might be functionally equivalent to the A83/F120 pair found in the Hck-activating HIV-1 N Nef proteins 02CM-DJO0131 and YBF106.

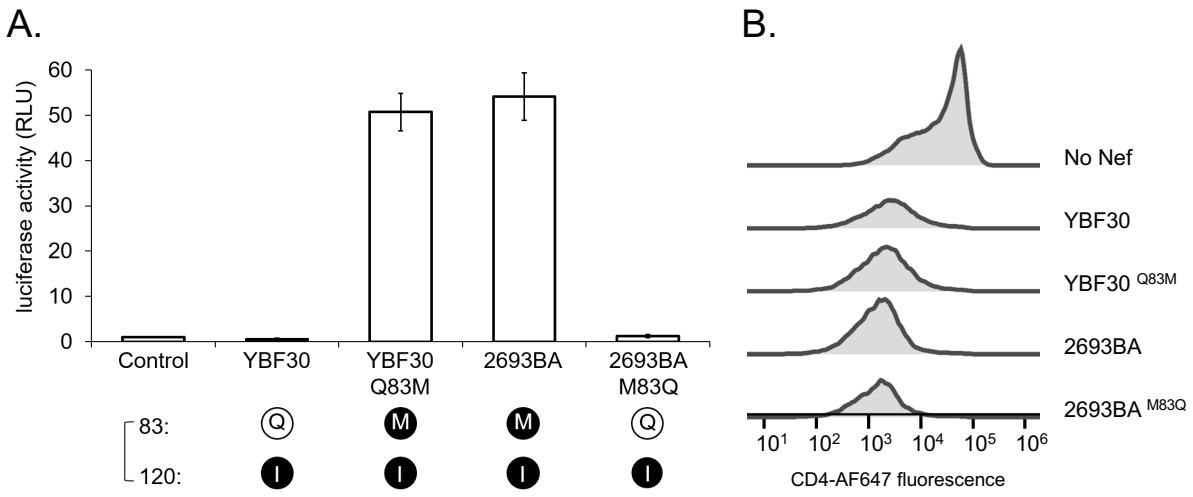

FIGURE 4: Role of residue 83/120 pairing in the HIV-1 N Nef R-clamp. (A) HZ-1 cells were transfected with an AP-1-dependent luciferase reporter alone (Control) or together with wild type (WT) versions of YBF30 or 2693BA Nef, or mutants thereof carrying reciprocal amino acid changes of residue 83 (YBF30 Q83M and 2693BA M83Q). Luciferase activity was measured from cells 4 h post-transfection, and normalized to the corresponding control sample that was set to one. The data shown are derived from three independent experiments, with SE indicated by error bars. The amino acid combinations

at positions 83 and 120 are indicated here and in the figures below as single-letter symbols and color-coded according to the residue classification shown in Table 1. Specifically, small (G or A) or hydrophilic residues (D, E, Q, or S) at position 83 are shown as a black 1-letter symbol in a white sphere (here Q83 in YBF30), whereas aliphatic or methionine residues at this position are shown as a white letter in a black sphere (here M83 in 2693BA). At position 120, aromatic residues (F or Y) are shown as a black letter in a white sphere (not found in YBF30 or 2693BA), whereas isoleucine is shown as a white letter in a black sphere (here I120 in YBF30 and 2693BA). **(B)** CD4 downregulation by Nef in stably transduced Jurkat T cells was examined as in Fig. 1C. Original dot plots are shown in Fig S2.

To test this idea, we swapped residues 83 between the I120-containing 2693BA and YBF30 Nef proteins. In line with our hypothesis, this reversed the differences in the Hck-activating capacity of these HIV-1 N Nefs, such that Nef-2693BA lost its ability to stimulate AP-1 activity, whereas YBF30 Nef became fully competent for this function (Figure 4). Thus, we conclude that Nef residues 83 and 120 appear to function together to form the R-clamp that coordinates Hck-SH3 binding by Nef, and that different combinations of residue pair 83/120 have evolved for building a functional R-clamp in HIV-1 group N Nefs.

Whereas among the Nef proteins of HIV-1, Ile can be found at position 120 only in group N viruses, we noted that several SIVcpz Nefs also contain Ile120 (Table 1). To test if our conclusions regarding the alternative R-clamp designs hold true also for SIVcpz Nef proteins, we examined five of these, three from SIV of the chimpanzee subspecies *Pan troglodytes troglodytes* (P.t.t.), namely MB897 (EF535994), CAM5 (AJ271369), and EK505 (DQ373065), and two from *Pan troglodytes schweinfurthii* (P.t.s.), namely Tan2 (EF394357) and Nok5 (AY536915).

We found that similar to the HIV-1 N YBF30 Nef, some of these SIVcpz Nefs (Cam5 and EK505) failed to activate Hck, whereas others (MB897, Nok5, and Tan2) were functional in this regard although all were able to downregulate CD4 (Figure 5). When the Hck activating capacity was compared with the residue 83/120 composition of these SIVcpz alleles, a perfect agreement was found with the structural R-clamp principles deduced from the results

obtained with HIV-1 N Nefs. All SIVcpz Nef proteins that were competent for Hck activation contained a "permissible" [83] + [120] residue combination defined as [tiny/hydrophilic] + [Phe/Tyr] or [aliphatic] + [Ile], whereas both of the two non-activating SIVcpz Nef proteins contained a mixed pattern of amino acid classes at these positions (Figures 2 and 5).

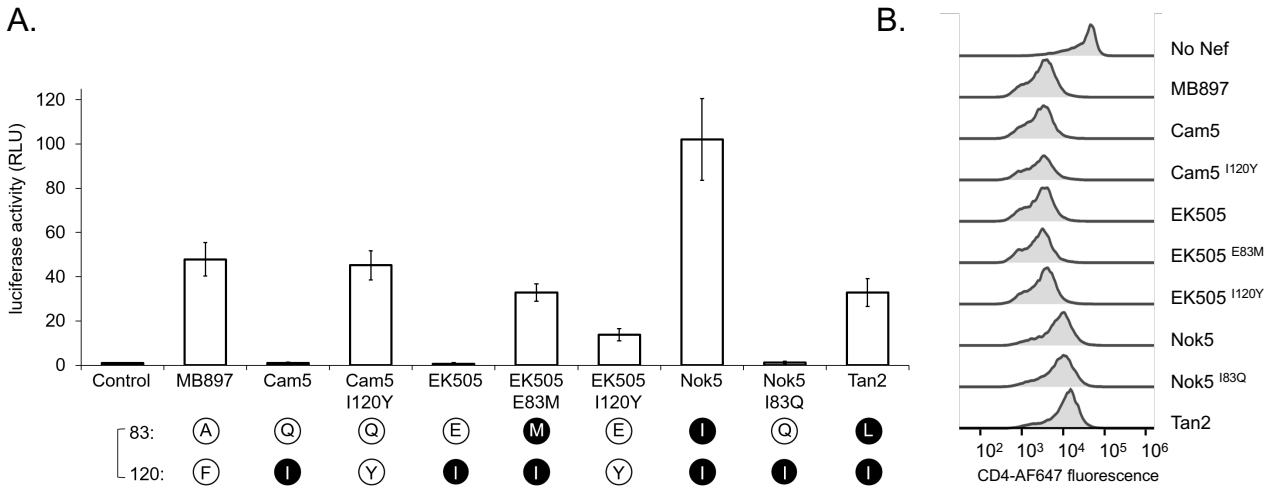

FIGURE 5: R-clamp architecture of SIVcpz Nef proteins. (A) HZ-1 cells were transfected with an AP-1-luciferase reporter alone (Control) or together with wild-type or the indicated mutants of Nef from SIV strains from *Pan troglodytes troglodytes* (MB897, Cam5, and EK505) or *Pan troglodytes schweinfurthii* (Nok5 and Tan2). Luciferase activity in the transfected lysates was analyzed as in Fig. 1C. The data shown are derived from three independent experiments, with SE indicated by error bars. The amino acid combinations at positions 83 and 120 are indicated as single-letter symbols and color-coded as explained in Fig. 4. **(B)** CD4 downregulation by Nef in stably transduced Jurkat T cells was examined as in Fig. 1C. Original dot plots are shown in Fig S3.

To further prove this concept, we showed that the failure of Cam5 and EK505 Nef to activate Hck could indeed be corrected by introducing a tyrosine residue at position 120 in these proteins, thereby providing them with an R-clamp residue combination 83 [hydrophilic] + 120 [Phe/Tyr]. Moreover, an E83M mutation (resulting in an 83 [aliphatic] + 120 [Ile] residue combination) conferred this activity to EK505 Nef. On the other hand, introducing a

hydrophilic residue at position 83 of Nok5 Nef while maintaining its Ile120 residue (Nok5 I83Q) led to a complete loss of its Hck-activating potential, as predicted by our model on the compatible and non-compatible R-clamp residue combinations.

Category	Residue 120	Residue 83	**HIV-1 M** n= 5221	**HIV-1 O** n= 56	**HIV-1 P** n= 4	**HIV-1 N** n= 12	**SIVcpz (p.t.t.)** n= 18	**SIVcpz (p.t.s.)** n= 12	**SIVgor** n= 6
I	F,Y	A,G	96.1 %	100 %	100 %	58.3 %	66.7 %	0 %	100 %
II	F,Y	D,E,Q,S	2.6 %	0 %	0 %	0 %	0 %	0 %	0 %
III	I	D,E,Q,S	0.5 %	0 %	0 %	25.0 %	33.3 %	0 %	0 %
IV	I	I,L,M,V	0.1 %	0 %	0 %	16.7 %	0 %	100%*	0 %

TABLE 1: R-clamp residue combinations in the HIV-1-like superfamily of Nef proteins. Altogether, 5329 HIV-1, SIVcpz, and SIVgor Nef sequences were classified into four categories (I – IV) based on the side chain properties of residues 83 and 120 as indicated. Individual HIV-1 M Nef proteins evading this classification could be found, but showed frequencies <0.05%. *Instead of Ile, some SIVcpz(P.t.s.) proteins contain Val at position 120.

When the residue 83/120 composition was analyzed in a comprehensive survey of HIV-1/SIVcpz/SIVgor Nef sequences, it was interesting to observe that the different evolutionary lineages of primate lentivirus are associated with distinct R-clamp design strategies. In Table 1, these strategies have been grouped into four categories (I – IV) based on the amino acid side chain properties explained above, and their occurrence has been calculated as a percentage of all Nef sequences found for each lentivirus lineage. Whereas HIV-1 M, HIV-1 O, HIV-1 P, and SIVgor viruses fall almost exclusively into category I, HIV-1 N and SIVcpz viruses show more heterogeneity. Interestingly, however, all SIVcpz Nef proteins from the chimpanzee subspecies P.t.s. fall into category IV, while all SIVcpz(P.t.t.) Nef proteins are found in categories I (67%) or III (33%). HIV-1 N Nef proteins share the R-clamp design patterns with SIVcpz(P.t.t.) and SIVcpz(P.t.s.), and can be found spread

between categories I, III, as well as IV. Finally, exclusively HIV-1 M Nef proteins can be found in category II, which includes a small but significant proportion (2.6%) of all the 5221 HIV-1 M Nef protein sequences in our survey.

Of note, the relative distribution of HIV-1 M Nef sequences into categories I to IV is not even between different viral subtypes. Whereas subtype B that constitutes more than half of all available HIV-1 M Nef sequences rarely falls in I120-containing categories III (0.31%) or IV (0.03%), this is much more common among subtype D and G Nef proteins, of which 2.91% and 2.59%, respectively belong to categories III or IV. And although only four of out the total 5221 HIV-1 M Nef sequences belong to category IV, two of these can be found among the 206 subtype D Nef sequences. On the other hand, while category II covers 2.6% of total HIV-1 M Nef sequences, this is the case for as many as 15.6% of subtype G and 7.1% of subtype H, but only 0.5% of subtype A strains.

Based on the experiments presented above it was inferred that Nef proteins in categories I, II, and IV can bind Hck to stimulate its tyrosine kinase activity, whereas category III Nef proteins with a "mixed" R-clamp residues pattern fail to do so. To further substantiate the generality of this conclusion, we introduced several additional individual and combinatorial 83/120 residue changes into the model Nef protein of HIV-1 M SF2 according to the classification presented in Table 1. We found that a Gln, Glu, or Ser residue could indeed all be introduced at position 83 of SF2-Nef without losing its Hck-activating function, as long as an aromatic residue was maintained at position 120 (Figure 6; SF2 A83Q, A83E, and A83S). Thus, all these different category II configurations could support a functional R-clamp when artificially introduced into SF2-Nef.

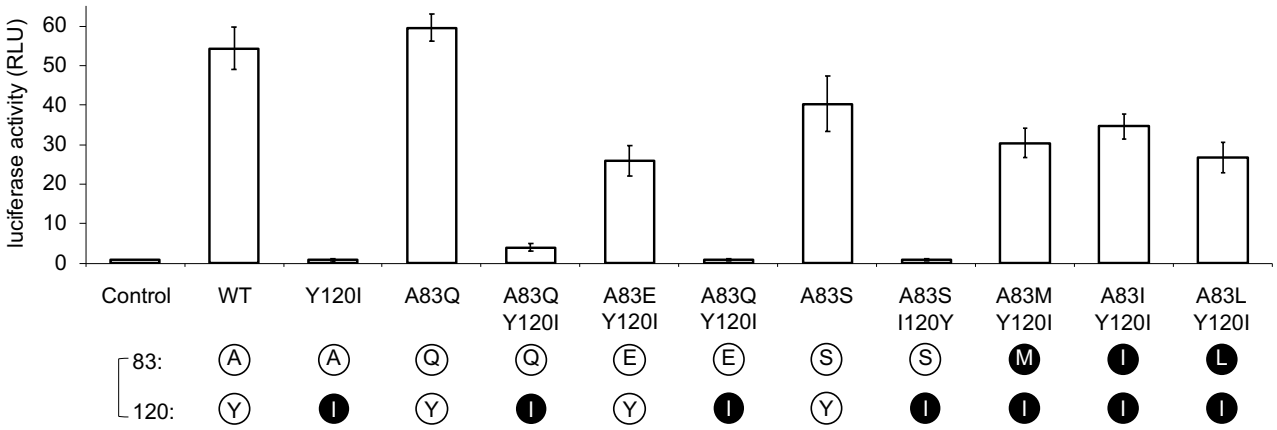

FIGURE 6: Comprehensive testing of R-clamp residue pairing rules by mutagenesis of SF2-Nef. Nef-induced AP-1 activity in cells transfected without Nef (Control) or with the indicated wild-type or mutant versions of SF2 Nef was analyzed as in Fig. 1B. The amino acid combinations at positions 83 and 120 of these SF2 Nef variants are indicated as single-letter symbols that are color-coded as explained in Fig. 4.

By contrast, and again in full agreement with our R-clamp model, combination of these mutations with an Y120I change to introduce a category III "mixed" residue 83/120 pattern into SF2 (Q83S/Y120I, A83S/Y120I, and A83E/Y120I) resulted in all three cases in the loss of Hck activation. Finally, the disrupted Hck-activating function of the single residue 120 mutant SF2 Y120I could be fully rescued via an additional introduction of Met, Ile, or Leu at position 83 to generate artificial category IV-like SF2 Nef double mutants A83M/Y120I ("2693BA-like"), A83I/Y120I ("Nok5-like"), and A83L/Y120I ("Tan2-like").

Together, these results provide strong further proof to our conclusions on the 83/120 residue combinations that are required for Hck binding and activation, and demonstrate interesting structural and evolutionary plasticity in organizing a set of molecular interactions via an R-clamp principle to enable Nef to tightly bind the SH3 domain of Hck.

DISCUSSION

Apart from the regulation of trafficking of CD4 and other membrane proteins, the majority of all cellular functions described for Nef depend on its SH3 domain binding capacity, and are lost if the highly conserved consensus SH3 ligand motif PxxPxR of Nef is mutated [7]. Here we show that Nef proteins of HIV-1 and closely related SIVs have evolved a sophisticated molecular mechanism that we have termed the R-clamp in order to coordinate their SH3 binding. This term was coined due to buttressing of the arginine residue of the Nef PxxPxR motif (R77) by the coordinated action of the Nef residues 83 and 120 together with a tryptophan residue (W37) that is conserved in almost all SH3 domains. This places R77 of Nef into close proximity with another highly conserved SH3 residue (D17) to form a salt bridge that stabilizes the Nef/SH3 complex. Thus, docking of proline-rich ligand peptides presented by native proteins, such as Nef, can involve an additional level of structural complexity for tuning of SH3 binding affinity and specificity that is not evident from studies with isolated SH3 binding peptides.

Our studies have focused on the SH3-mediated interaction between Nef and the tyrosine kinase Hck leading to enzymatic activation of Hck, which we have monitored based on induction of downstream signaling events, including paxillin phosphorylation as well as triggering of the Raf/MAPK cascade and subsequent AP-1-regulated gene expression. Nef/Hck interaction is thought to play an important role in HIV infection of cells of the myeloid lineages, such as macrophages, and is an especially tractable study system because of the high affinity of Hck SH3 domain for Nef [19]. This is due to the additional affinity brough into this interaction by tertiary contacts outside of the canonical SH3 ligand binding surface and involving the tip of the RT-loop in Hck SH3 [9, 25]. Because of the lack of such RT-loop contacts, SH3 domains of other host cell proteins bind to Nef with a lower affinity resulting in more transient interactions that have remained less well characterized, but

appear to include at least Lck [26], Vav [27], PACS-1 [28], Btk, and Itk [29]. Nevertheless, similar to Hck-binding, all SH3 interactions by Nef are expected to depend on formation of a salt bridge between R77 of Nef and acidic (D or E) SH3 residue 17. Thus, all these interactions, including the SH3-mediated complexes that are relevant for Nef in T lymphocytes depend on a functional R-clamp.

Interestingly, we found that in different lentiviral Nef proteins the R-clamp has been assembled based on alternative designs, which depend on the combination of amino acids at positions 83 and 120. Moreover, the preferred 83/120 residue combinations are dissimilar in different lineages of HIV-1, SIVcpz, and SIVgor (Table 1). While the vast majority of HIV-1 group M, O and P Nefs belongs to category I, HIV-1 N Nefs are more heterogenous and fall into categories I or IV (harboring an active R-clamp) or inactive category III (Figure 7). Why would about 25% of all HIV-1 N Nefs harbor an inactive R-clamp, whereas their counterparts from HIV-1 groups M, O, and P do not? Since SIVcpz(P.t.t.), the simian precursor of HIV-1, comprises category I and III Nefs, it is tempting to speculate that the zoonotic transmission that gave rise to HIV-1 group N involved a virus carrying a Nef with a category III R-clamp.

In line with this hypothesis, the inferred common ancestor of HIV-1 group N viruses belongs to category III as its Nef protein harbors a combination of Q83 and I120 [30](GenBank accession: KP059120.1). Furthermore, the SIVcpz(P.t.t.) isolate EK505 (DQ373065), a close relative of HIV-1 group N viruses [31] also expresses a category III Nef. Thus, HIV-1 group N viruses may all be the result of a category III virus, and still be adapting and evolving into categories I and IV with functional R-clamps. Notably, group N most likely represents the evolutionarily youngest of all HIV-1 groups [32, 33], and the three most recently isolated group N Nefs (JN572926, MF767262, KY498771), including that of N1_FR_2011, the only group N virus isolated outside Cameroon [34], belong to categories I or IV. A single amino acid change of residue 83 (like the EK505-E83M mutant created in this study; see Fig. 5) would

have been sufficient to move from category III to IV, whereas the path from category III to I would require changes in both residues 83 and 120, and thus follow an evolutionary trajectory via category II. None of the currently available HIV-1 N Nef sequences fall into the R-clamp category II, but given the scarcity (n=12) of these sequences this does not mean that such HIV-1 N Nefs could still not exist.

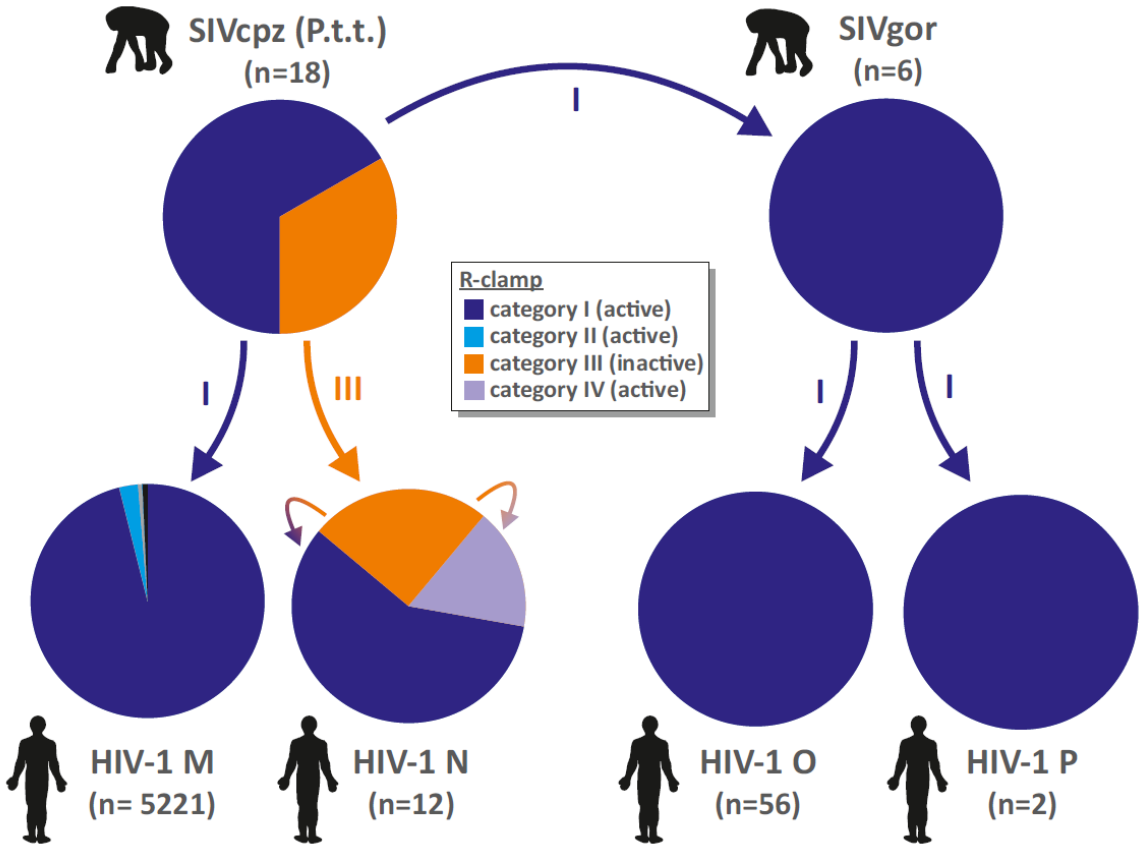

FIGURE 7: Prevalence of R-clamp categories in HIV-1 groups M, N, O and P, as well as SIVcpz and SIVgor and their putative cross-species transmission. Pie charts illustrating the relative fraction of R-clamp categories I-IV in HIV-1 and its simian precursors. Inferred most recent common ancestors (MRCA) suggest that SIVgor and HIV-1 group M originated from a category I SIVcpz(P.t.t.), while a category III SIVcpz(P.t.t.) most likely gave rise to HIV-1 group N. This MRCA of HIV-1 N may subsequently have evolved into category I and III viruses.

In contrast to HIV-1 N, group M viruses almost exclusively fall into category I, suggesting that the zoonotic jump from SIVcpz(P.t.t) to HIV-1 M involved a virus with a category I Nef R-clamp. Indeed, the inferred most recent common ancestor of HIV-1 M Nefs (KP059118.1; KP059119.1; [30] belongs to category I. This is also true for the oldest known HIV-1 M Nef (M15896) isolated in 1976 [35]. Finally, the exclusive use of category I R-clamp by Nef proteins of SIVgor, HIV-1 O, and HIV-1 P would suggest that an R-clamp category I virus might have originally been transmitted from chimpanzee to gorilla, and subsequently in two independent cross-species jumps entered humans, giving rise to HIV-1 O and HIV-1 P.

It is of interest to note that a subtype D virus of the HIV-1 M group has been previously shown to encode a Nef protein unable to activate Hck, and that this deficiency was mapped to the unusual presence of an isoleucine residue at the Nef position 120 [36]. This study suggested that Tyr120 would contribute to the hydrophobic pocket of Nef that accommodates the Hck SH3 domain RT-loop, whereas I120 could not serve this function. However, these molecular contacts inferred based on our (NL4-3) Nef/SH3 X-ray structure (1EFN; [9]}) would be expected to only minor rather than critical for the Nef-Hck interaction, and a recent SH3 complex structure involving HIV-1 SF2 Nef [36] does not support such a role for Y120 at all. Moreover, our current data clearly show that category IV Nef proteins containing I120 do bind and activate Hck when paired with an appropriately matched R-clamp residue at the position 83. Thus, while the findings of Choi and Smithgall on Nef from HIV-1 ELI [36] are in agreement with our data, they need to be interpreted in light of the R-clamp concept described here.

While the evolutionary scenarios discussed above may help to explain the occurrence of inactive category III Nefs in HIV-1 group N, it still remains unclear why about one third of all SIVcpz(Pt.t.) Nefs harbor a category III R-clamp. Furthermore, the reasons for the unique predominance of category IV Nefs in SIVcpz(P.t.s.) remain to be determined. Apart from the

initial founder viruses that gave rise to the respective lentiviral lineages and species, the optimal R-clamp composition and the rate of R-clamp sequence evolution are probably determined by a complex balance between host-specific factors and sequence variation elsewhere in these viruses. To gain further insights, it would be interesting to examine a larger number of HIV-1 N Nef sequences over time and from different tissues from the same individual to understand whether the R-clamp pattern is relatively fixed or subject to rapid evolution and quasispecies variation. In the latter case, because of the highly multifunctional nature of the Nef protein, a non-functional R-clamp might provide a selective advantage in certain circumstances or anatomic locations. On the other hand, considering that an intact SH3 binding motif PxØPxR (where Ø is a hydrophobic residue, almost invariable a valine) is universally conserved, including Nef proteins with a category III R-clamp, it is also possible that while unable to interact with canonical SH3 domains, these Nef proteins might instead have an unusual specificity for certain atypical SH3 proteins, which could provide them with alternative cellular functions.

In any case, R-clamp sequence variation provides a fascinating example of evolutionary plasticity of a protein interaction interface and our findings suggest that the selection pressures that have shaped Nef during primate lentiviral evolution are different depending on the HIV/SIV lineage and their host species. The dynamic capacity of Nef for altering the molecular strategy of recognizing its key host cell interaction partners, such as SH3 domains, is also important to keep in mind in attempts to develop novel HIV eradication therapies that might target the immune evasion function of Nef.

MATERIALS AND METHODS

Reagents and cell lines

Mouse anti-Myc (sc-40) and rabbit anti-paxillin (sc-5574) were from Santa Cruz Biotechnology. Mouse anti-pY31 paxillin was from BD Biosciences. Alexa Fluor 647 conjugated anti-human CD4 antibody was from SouthernBiotech. IRDye680CW goat anti-mouse IgG, and IRDye800CW goat anti-rabbit IgG were from Li-Cor Biotechnology. HEK293 cells and Jurkat cells were obtained from ATCC. The derivation and characterization of the HEK293-based Hck-expressing HZ-1 cells have been described elsewhere [19]. HEK293 and HZ1 cells were grown in high-glucose Dulbecco's modified Eagle's medium (DMEM; Sigma) supplemented with 10% fetal bovine serum (FBS), 0.05 mg/ml penicillin, and 0.05mg/ml streptomycin. Lentiviral transduction was employed to generate Jurkat cells stably expressing human CD4. Briefly, HEK293 cells were co-transfected with 2.5 μg pDelta8.9, 1.5 μg VSV-G and 3 μg pWPI-puro plasmid containing human CD4 cDNA in Opti-MEM medium with 12 μg PEI. After 5 hours, medium was refreshed with cell culture media. Supernatant was collected 48 hours post-transfection, filtered and used to infect Jurkat cells. Infected cells were selected with 6 μg/ml puromycin for 2 days. Single cell clones of CD4 transduced Jurkat cells were isolated by cellenONE X1 system. Jurkat cells were maintained in RPMI-1640 medium (Sigma) supplemented with 10% FBS, 0.05 mg/ml penicillin, and 0.05 mg/ml streptomycin.

Plasmids

Nef alleles from HIV-1 M SF2 (P03407), HIV-1 N 2693BA (GQ925928), HIV-1 N S4858 (KY498771), HIV-1 N YBF30 (AJ006022), HIV-1 N YBF106 (AJ271370), HIV-1 N DJO0131 (AY532635), HIV-1 O 13127k4 (AY536904), HIV-1 P RBF168 (GU111555), SIVcpz(P.t.t) CAM5 (AJ271369), SIVcpz(P.t.t) EK505 (DQ373065), SIVcpz(P.t.t) MB897 (EF535994), SIVcpz(P.t.s)

ch-Nok5 (AY536915) and SIVcpz(P.t.s) Tan2 (EF394357) were cloned into the expression vector pEBB containing a C-terminal Myc-tag. The Nef mutants (HIV-1 M SF2 Y120F, Y120I, A83E, A83E/Y120I, A83I, A83I/Y120I, A83L, A83L/Y120I, A83M, A83M/Y120I, A83Q, A83Q/Y120I, A83S, A83S/Y120I; HIV-1 N YBF30 Q83M, YBF30 I120Y, 2693BA M83Q; SIVcpz(P.t.t) Cam5 I120Y, EK505 E83M, EK505 I120Y and SIVcpz (P.t.s) ch-Nok5 I83Q, ch-Nok5 I120F) were generated in the same vector backbone using standard PCR-assisted mutagenesis. The Nef variants (HIV-1 M SF2 wt, Y120F, Y120I; HIV-1 N DJO0131, HIV-1 N YBF116, HIV-1 N YBF30, HIV-1 O 13127k4, and HIV-1 P RBF168) were cloned into the pWPI-GFP vector (Addgene # 12254) to transduce Jurkat cells stably expressing CD4.

Immunoblots

Cells were collected and lysed on ice for 10 minutes in lysis buffer (150 mM NaCl, 50 mM Tris-HCl [pH 7.4], 1% NP-40) with protease and phosphatase inhibitors (Thermo Fisher Scientific). Cell lysates were centrifuged at 16,000 x g at 4°C for 5 min. Proteins from cell extracts were analyzed by standard SDS gel electrophoresis and Western blotting using IRDye-labeled detection reagents detailed above.

AP-1 luciferase reporter assay.

HZ1 cells were transfected using TransIT-2020 reagent (Mirus) with 50 ng of Nef expression vector together with 50 ng of AP-1 pfLUC reporter plasmid [37] driving the AP-1 inducible expression of firefly luciferase, plus 50 ng of the plasmid pRL-TK (Promega) expressing low and constitutive levels of *Renilla* luciferase. Cells were collected and lysed with lysis buffer (Promega) on ice. A dual-luciferase reporter assay system from Promega was utilized to determine luciferase activities following the manufacturer's protocol using Berthold Sirius single-tube luminometer detection.

Transduction of Jurkat cells and flow cytometry analysis of CD4

Nef-expressing HIV-1-like pseudoviruses were produced as described previously [19]. Jurkat cells stably expressing CD4 were infected with such lentiviral vectors containing various *nef* alleles. 3 days post-infection the cells were collected and washed twice with PBS (pH 7.4), followed by fixing with 1% Paraformaldehyde (Sigma) at room temperature for 20 min. Cells were washed twice with PBS containing 2% FBS (FACS buffer) and stained with Alexa Fluor 647 conjugated anti human CD4 antibody at room temperature for 40 min. After staining the cells were washed twice with FACS buffer and re-suspended in PBS. The CD4 cell surface expression was analyzed using a BD Accuri C6 flow cytometer (BD Biosciences) and data analysis was performed using FlowJo software (version 10.4, Ashland OR: Becton, Dickinson and Company).

ACKNOWLEDGMENTS

We thank Ms. Virpi Syvälahti for expert technical assistance. This study was supported by grants to KS from the Helsinki University Central Hospital Research Council and the Jane and Aatos Erkko Foundation. DS was supported by the Heisenberg Program and the Priority Program SPP1923 of the German Research Foundation (DFG). We acknowledge CSC-IT Center for Science Ltd. for the allocation of computational resources. The authors have no conflicts of interest to disclose.

REFERENCES

1. Sauter D, Kirchhoff F. Key Viral Adaptations Preceding the AIDS Pandemic. Cell host & microbe. 2019;25(1):27-38. Epub 2019/01/11. doi: 10.1016/j.chom.2018.12.002. PubMed PMID: 30629915.

2. Désiré N, Cerutti L, Le Hingrat Q, Perrier M, Emler S, Calvez V, et al. Characterization update of HIV-1 M subtypes diversity and proposal for subtypes A and D sub-subtypes reclassification. Retrovirology. 2018;15(1):80. Epub 2018/12/24. doi: 10.1186/s12977-018-0461-y. PubMed PMID: 30577842; PubMed Central PMCID: PMCPMC6303845.

3. Robertson DL, Anderson JP, Bradac JA, Carr JK, Foley B, Funkhouser RK, et al. HIV-1 nomenclature proposal. Science (New York, NY). 2000;288(5463):55-6. Epub 2000/04/15. doi: 10.1126/science.288.5463.55d. PubMed PMID: 10766634.

4. Yamaguchi J, Vallari A, McArthur C, Sthreshley L, Cloherty GA, Berg MG, et al. Brief Report: Complete Genome Sequence of CG-0018a-01 Establishes HIV-1 Subtype L. Journal of acquired immune deficiency syndromes (1999). 2020;83(3):319-22. Epub 2019/11/07. doi: 10.1097/qai.0000000000002246. PubMed PMID: 31693506; PubMed Central PMCID: PMCPMC7012332 Laboratories. The remaining authors have no conflicts of interest to disclose.

5. Kirchhoff F, Schindler M, Specht A, Arhel N, Munch J. Role of Nef in primate lentiviral immunopathogenesis. Cellular and molecular life sciences : CMLS. 2008;65(17):2621-36. Epub 2008/04/29. doi: 10.1007/s00018-008-8094-2. PubMed PMID: 18438604.

6. Arhel NJ, Kirchhoff F. Implications of Nef: host cell interactions in viral persistence and progression to AIDS. Current topics in microbiology and immunology.

2009;339:147-75. Epub 2009/12/17. doi: 10.1007/978-3-642-02175-6_8. PubMed PMID: 20012528.

7. Saksela K. Interactions of the HIV/SIV pathogenicity factor Nef with SH3 domain-containing host cell proteins. Current HIV research. 2011;9(7):531-42. Epub 2011/11/23. PubMed PMID: 22103837.

8. Staudt RP, Alvarado JJ, Emert-Sedlak LA, Shi H, Shu ST, Wales TE, et al. Structure, function, and inhibitor targeting of HIV-1 Nef-effector kinase complexes. The Journal of biological chemistry. 2020;295(44):15158-71. Epub 2020/08/31. doi: 10.1074/jbc.REV120.012317. PubMed PMID: 32862141; PubMed Central PMCID: PMCPMC7606690.

9. Lee CH, Saksela K, Mirza UA, Chait BT, Kuriyan J. Crystal structure of the conserved core of HIV-1 Nef complexed with a Src family SH3 domain. Cell. 1996;85(6):931-42. Epub 1996/06/14. doi: 10.1016/s0092-8674(00)81276-3. PubMed PMID: 8681387.

10. Moarefi I, LaFevre-Bernt M, Sicheri F, Huse M, Lee CH, Kuriyan J, et al. Activation of the Src-family tyrosine kinase Hck by SH3 domain displacement. Nature. 1997;385(6617):650-3. Epub 1997/02/13. doi: 10.1038/385650a0. PubMed PMID: 9024665.

11. Guiet R, Poincloux R, Castandet J, Marois L, Labrousse A, Le Cabec V, et al. Hematopoietic cell kinase (Hck) isoforms and phagocyte duties - from signaling and actin reorganization to migration and phagocytosis. European journal of cell biology. 2008;87(8-9):527-42. Epub 2008/06/10. doi: 10.1016/j.ejcb.2008.03.008. PubMed PMID: 18538446.

12. Kumar A, Herbein G. The macrophage: a therapeutic target in HIV-1 infection. Molecular and cellular therapies. 2014;2:10. Epub 2014/01/01. doi: 10.1186/2052-8426-2-10. PubMed PMID: 26056579; PubMed Central PMCID: PMCPMC4452058.

13. Greenberg ME, Iafrate AJ, Skowronski J. The SH3 domain-binding surface and an acidic motif in HIV-1 Nef regulate trafficking of class I MHC complexes. Embo j. 1998;17(10):2777-89. Epub 1998/06/10. doi: 10.1093/emboj/17.10.2777. PubMed PMID: 9582271; PubMed Central PMCID: PMCPMC1170618.

14. Imle A, Abraham L, Tsopoulidis N, Hoflack B, Saksela K, Fackler OT. Association with PAK2 Enables Functional Interactions of Lentiviral Nef Proteins with the Exocyst Complex. mBio. 2015;6(5):e01309-15. Epub 2015/09/10. doi: 10.1128/mBio.01309-15. PubMed PMID: 26350970; PubMed Central PMCID: PMCPMC4600113.

15. Rudolph JM, Eickel N, Haller C, Schindler M, Fackler OT. Inhibition of T-cell receptor-induced actin remodeling and relocalization of Lck are evolutionarily conserved activities of lentiviral Nef proteins. J Virol. 2009;83(22):11528-39. Epub 2009/09/04. doi: 10.1128/jvi.01423-09. PubMed PMID: 19726522; PubMed Central PMCID: PMCPMC2772722.

16. Saksela K, Cheng G, Baltimore D. Proline-rich (PxxP) motifs in HIV-1 Nef bind to SH3 domains of a subset of Src kinases and are required for the enhanced growth of Nef+ viruses but not for down-regulation of CD4. EMBO J. 1995;14(3):484-91. Epub 1995/02/01. PubMed PMID: 7859737; PubMed Central PMCID: PMC398106.

17. Mayer BJ. The discovery of modular binding domains: building blocks of cell signalling. Nature reviews Molecular cell biology. 2015;16(11):691-8. Epub 2015/10/01. doi: 10.1038/nrm4068. PubMed PMID: 26420231.

18. Saksela K, Permi P. SH3 domain ligand binding: What's the consensus and where's the specificity? FEBS Lett. 2012;586(17):2609-14. Epub 2012/06/20. doi: 10.1016/j.febslet.2012.04.042. PubMed PMID: 22710157.

19. Zhao Z, Fagerlund R, Baur AS, Saksela K. HIV-1 Nef-induced secretion of the proinflammatory protease TACE into extracellularvesicles is mediated by Raf-1, and can be

suppressed by clinical protein kinase inhibitors. J Virol. 2021. Epub 2021/02/19. doi: 10.1128/jvi.00180-21. PubMed PMID: 33597213.

20. Collette Y, Arold S, Picard C, Janvier K, Benichou S, Benarous R, et al. HIV-2 and SIV nef proteins target different Src family SH3 domains than does HIV-1 Nef because of a triple amino acid substitution. The Journal of biological chemistry. 2000;275(6):4171-6. Epub 2000/02/08. doi: 10.1074/jbc.275.6.4171. PubMed PMID: 10660579.

21. Zhao Z, Kesti T, Uğurlu H, Baur AS, Fagerlund R, Saksela K. Tyrosine phosphorylation directs TACE into extracellular vesicles via unconventional secretion. Traffic (Copenhagen, Denmark). 2019;20(3):202-12. Epub 2018/12/21. doi: 10.1111/tra.12630. PubMed PMID: 30569492.

22. Kirchhoff F, Schindler M, Bailer N, Renkema GH, Saksela K, Knoop V, et al. Nef proteins from simian immunodeficiency virus-infected chimpanzees interact with p21-activated kinase 2 and modulate cell surface expression of various human receptors. J Virol. 2004;78(13):6864-74. Epub 2004/06/15. doi: 10.1128/jvi.78.13.6864-6874.2004. PubMed PMID: 15194762; PubMed Central PMCID: PMC421647.

23. Pettersen EF, Goddard TD, Huang CC, Couch GS, Greenblatt DM, Meng EC, et al. UCSF Chimera--a visualization system for exploratory research and analysis. Journal of computational chemistry. 2004;25(13):1605-12. Epub 2004/07/21. doi: 10.1002/jcc.20084. PubMed PMID: 15264254.

24. Case DA, Belfon K, Ben-Shalom IY, Brozell SR, Cerutti DS, Cheatham TEI, et al. AMBER 2020: University of California, San Francisco; 2020.

25. Hiipakka M, Poikonen K, Saksela K. SH3 domains with high affinity and engineered ligand specificities targeted to HIV-1 Nef. J Mol Biol. 1999;293(5):1097-106. Epub 1999/11/05. doi: 10.1006/jmbi.1999.3225. PubMed PMID: 10547288.

26. Collette Y, Dutartre H, Benziane A, Ramos M, Benarous R, Harris M, et al. Physical and functional interaction of Nef with Lck. HIV-1 Nef-induced T-cell signaling defects. The Journal of biological chemistry. 1996;271(11):6333-41. Epub 1996/03/15. doi: 10.1074/jbc.271.11.6333. PubMed PMID: 8626429.

27. Rauch S, Pulkkinen K, Saksela K, Fackler OT. Human immunodeficiency virus type 1 Nef recruits the guanine exchange factor Vav1 via an unexpected interface into plasma membrane microdomains for association with p21-activated kinase 2 activity. J Virol. 2008;82(6):2918-29. Epub 2007/12/21. doi: 10.1128/jvi.02185-07. PubMed PMID: 18094167; PubMed Central PMCID: PMCPMC2259019.

28. Blagoveshchenskaya AD, Thomas L, Feliciangeli SF, Hung CH, Thomas G. HIV-1 Nef downregulates MHC-I by a PACS-1- and PI3K-regulated ARF6 endocytic pathway. Cell. 2002;111(6):853-66. Epub 2003/01/16. doi: 10.1016/s0092-8674(02)01162-5. PubMed PMID: 12526811.

29. Tarafdar S, Poe JA, Smithgall TE. The accessory factor Nef links HIV-1 to Tec/Btk kinases in an Src homology 3 domain-dependent manner. The Journal of biological chemistry. 2014;289(22):15718-28. Epub 2014/04/12. doi: 10.1074/jbc.M114.572099. PubMed PMID: 24722985; PubMed Central PMCID: PMCPMC4140925.

30. Kluge SF, Mack K, Iyer SS, Pujol FM, Heigele A, Learn GH, et al. Nef proteins of epidemic HIV-1 group O strains antagonize human tetherin. Cell host & microbe. 2014;16(5):639-50. Epub 2014/12/20. doi: 10.1016/j.chom.2014.10.002. PubMed PMID: 25525794; PubMed Central PMCID: PMCPMC4274627.

31. Bibollet-Ruche F, Heigele A, Keele BF, Easlick JL, Decker JM, Takehisa J, et al. Efficient SIVcpz replication in human lymphoid tissue requires viral matrix protein adaptation. The Journal of clinical investigation. 2012;122(5):1644-52. Epub 2012/04/17. doi: 10.1172/jci61429. PubMed PMID: 22505456; PubMed Central PMCID: PMCPMC3336991.

32. Sauter D, Hué S, Petit SJ, Plantier JC, Towers GJ, Kirchhoff F, et al. HIV-1 Group P is unable to antagonize human tetherin by Vpu, Env or Nef. Retrovirology. 2011;8:103. Epub 2011/12/17. doi: 10.1186/1742-4690-8-103. PubMed PMID: 22171785; PubMed Central PMCID: PMCPMC3285029.

33. Wertheim JO, Worobey M. Dating the age of the SIV lineages that gave rise to HIV-1 and HIV-2. PLoS computational biology. 2009;5(5):e1000377. Epub 2009/05/05. doi: 10.1371/journal.pcbi.1000377. PubMed PMID: 19412344; PubMed Central PMCID: PMCPMC2669881.

34. Delaugerre C, De Oliveira F, Lascoux-Combe C, Plantier JC, Simon F. HIV-1 group N: travelling beyond Cameroon. Lancet (London, England). 2011;378(9806):1894. Epub 2011/11/29. doi: 10.1016/s0140-6736(11)61457-8. PubMed PMID: 22118443.

35. Srinivasan A, York D, Butler D, Jr., Jannoun-Nasr R, Getchell J, McCormick J, et al. Molecular characterization of HIV-1 isolated from a serum collected in 1976: nucleotide sequence comparison to recent isolates and generation of hybrid HIV. AIDS research and human retroviruses. 1989;5(2):121-9. Epub 1989/04/01. doi: 10.1089/aid.1989.5.121. PubMed PMID: 2713163.

36. Aldehaiman A, Momin AA, Restouin A, Wang L, Shi X, Aljedani S, et al. Synergy and allostery in ligand binding by HIV-1 Nef. The Biochemical journal. 2021;478(8):1525-45. Epub 2021/04/01. doi: 10.1042/bcj20201002. PubMed PMID: 33787846; PubMed Central PMCID: PMCPMC8079166.

37. Pesu M, Takaluoma K, Aittomaki S, Lagerstedt A, Saksela K, Kovanen PE, et al. Interleukin-4-induced transcriptional activation by stat6 involves multiple serine/threonine kinase pathways and serine phosphorylation of stat6. Blood. 2000;95(2):494-502. Epub 2000/01/11. PubMed PMID: 10627454.

38. Gallivan JP, Dougherty DA. Cation-pi interactions in structural biology. Proceedings of the National Academy of Sciences of the United States of America. 1999;96(17):9459-64. Epub 1999/08/18. doi: 10.1073/pnas.96.17.9459. PubMed PMID: 10449714; PubMed Central PMCID: PMCPMC22230.

39. Gómez-Tamayo JC, Cordomí A, Olivella M, Mayol E, Fourmy D, Pardo L. Analysis of the interactions of sulfur-containing amino acids in membrane proteins. Protein science : a publication of the Protein Society. 2016;25(8):1517-24. Epub 2016/05/31. doi: 10.1002/pro.2955. PubMed PMID: 27240306; PubMed Central PMCID: PMCPMC4972207.

40. Berendsen HJC, Postma JPM, van Gunsteren WF, DiNola A, Haak JR. Molecular dynamics with coupling to an external bath. The Journal of chemical physics. 1984;81:3684–90. doi: 10.1063/1.448118.

41. Darden T, York D, Pedersen L. Particle mesh Ewald: an N·log(N) method for Ewald sums in large systems. The Journal of chemical physics. 1993;98:10089–92. doi: 10.1063/1.464397.

42. Ryckaert J-P, Ciccotti G, Berendsen HJC. Numerical integration of the cartesian equations of motion of a system with constraints: molecular dynamics of n-alkanes. J Comput Phys. 1977;23:327-41. doi: 10.1016/0021-9991(77)90098-5.

43. Roe DR, Cheatham TE, 3rd. PTRAJ and CPPTRAJ: Software for Processing and Analysis of Molecular Dynamics Trajectory Data. Journal of chemical theory and computation. 2013;9(7):3084-95. Epub 2013/07/09. doi: 10.1021/ct400341p. PubMed PMID: 26583988.

SUPPLEMENTARY FIGURE 1

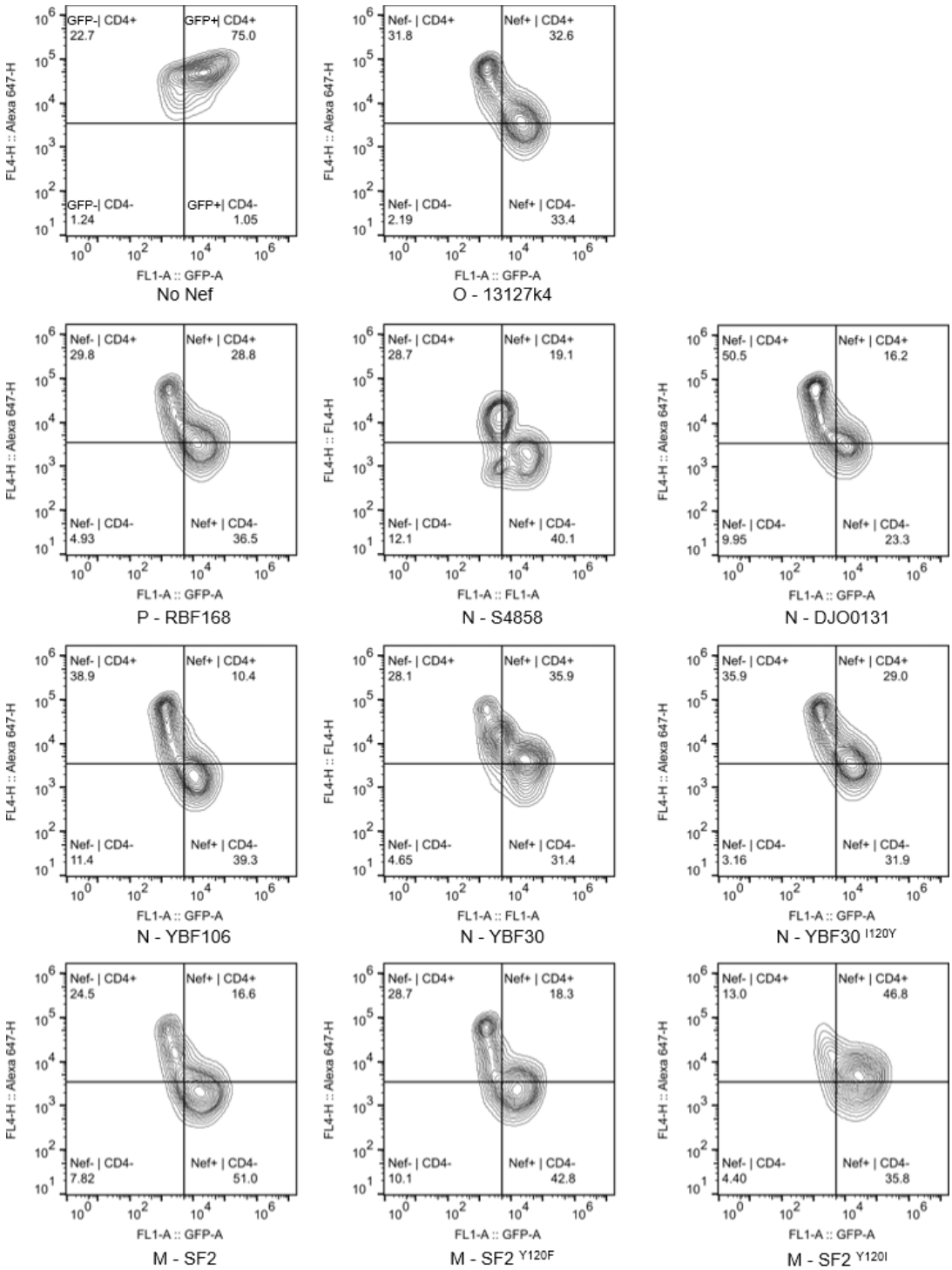

Raw data for histograms shown in Figure 1C

SUPPLEMENTARY FIGURE 2

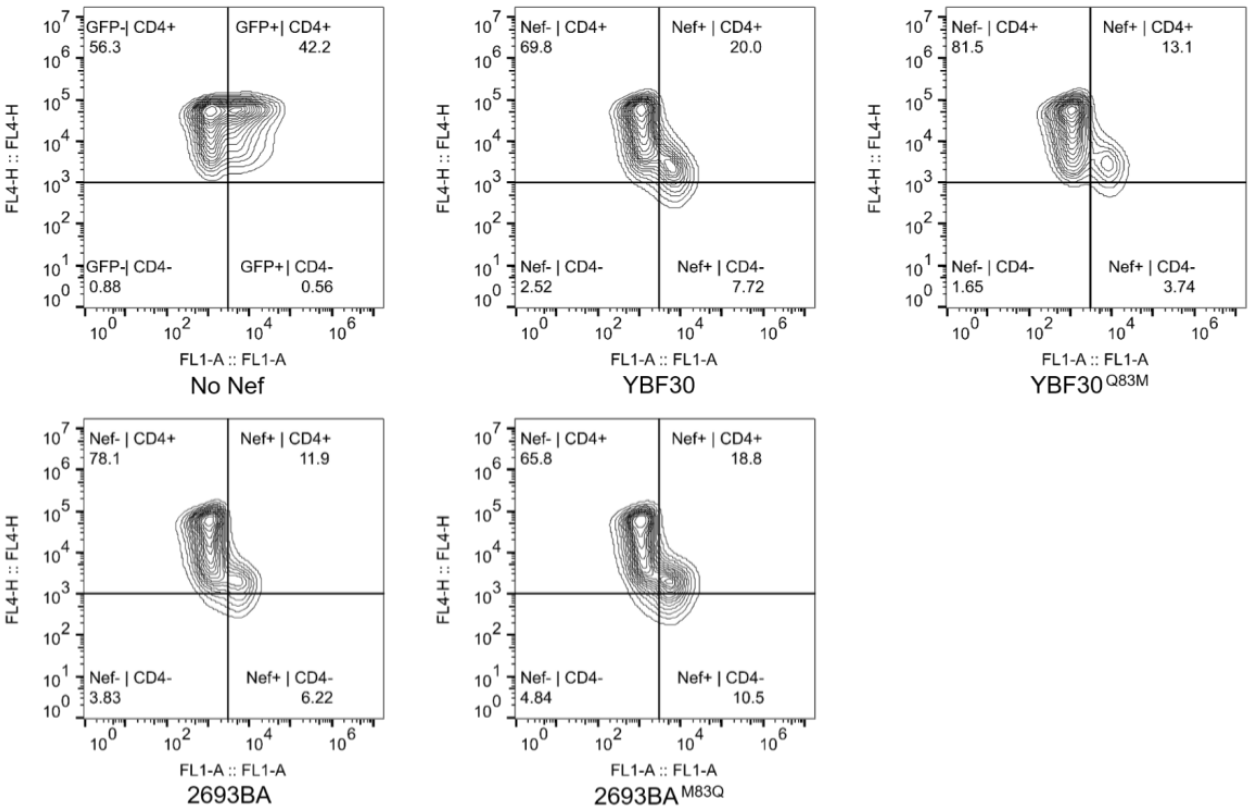

Raw data for histograms shown in Figure 4B

SUPPLEMENTARY FIGURE 3

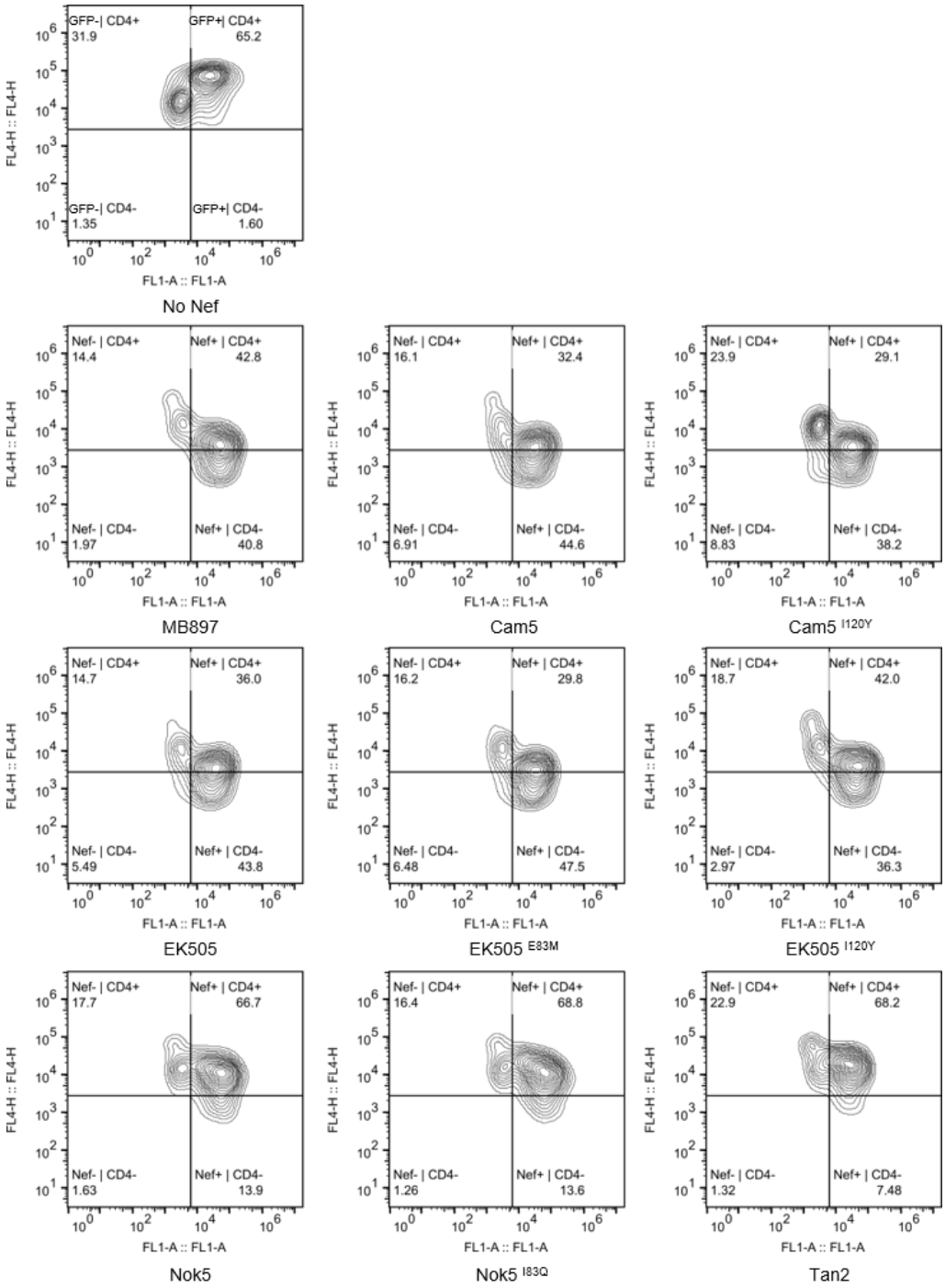

Raw data for histograms shown in Figure 5B

SUPPLEMENTARY FIGURE 4

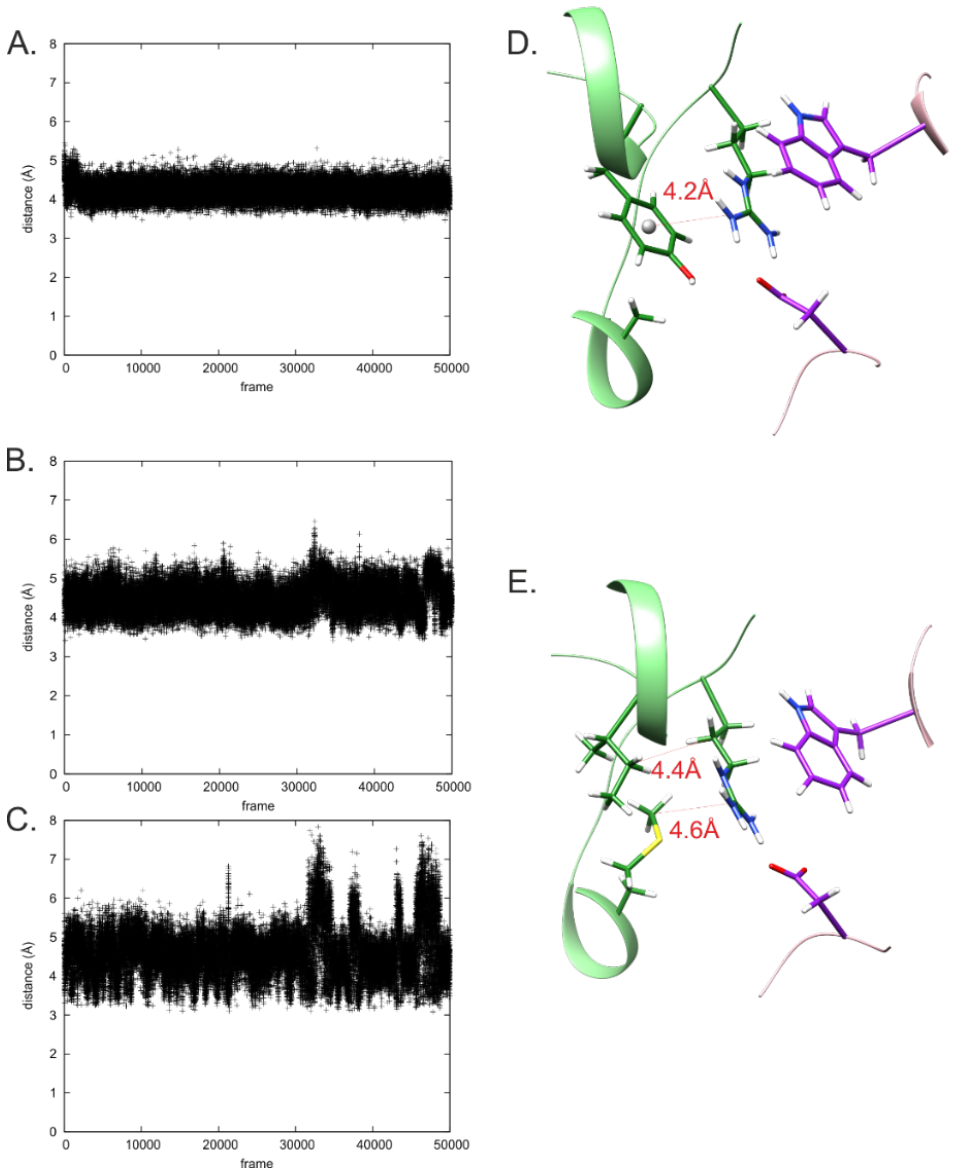

One-hundred ns all-atom molecular dynamics simulations show that stabilization of R77 side chain provided by the R-clamp in the wild-type complex could be reproduced by Met, Ile and Trp in the A83M/Y120I double mutant. Analysis of the MD trajectories show that in the wild type complex the stacked Tyr-Arg-Trp π-cation-π interaction remains stable, as interpreted from Arg to Tyr and Arg to Trp side chain distances, which show little fluctuations around their average values, 4.2 Å **(A)** and 3.5 Å **(B)**. In **(C)** is shown a snapshot from the wild type complex simulation in which these distances are close to their average values. In the double mutant the Arg to Trp distance is on the average about

0.5 Å longer than that in the wild type complex **(E)**, but also remains stable around its average value, 4.0 Å. If 6 Å is taken as the maximum distance for a cation-π interaction [38] the observed distances are well within the limit. Likewise, hydrophobic contacts to and between Met and Ile on the other side of the Arg plane remain relatively stable. Non-bonded contacts are likely to be bolstered by Met sulfur [39]. Ile and Arg sidechains are on average 4.4 Å apart **(D)**. Met to Arg **(F)** and Ile to Met **(G)** distances show more variation, but are for the majority of time close to about 4.6 and 3.9 Å. In **(H)** is shown a snapshot from the double mutant complex simulation in which these distances are close to their average values. A salt bridge between Arg and Asp side chains is present in 96 % (WT) and 93% (double mutant) of the simulation frames. MD simulations in explicit solvent were performed with AMBER 20 [24] using the ff14SB force field. The WT and A83M/Y120I complexes were placed in a cubic box with a minimum solute-box distance of 10 Å, and solvated with TIP3P water molecules. Six sodium ions were added to neutralize the system. After minimization, heating and equilibration of the system, the production 100-ns MD simulations were performed with periodic boundary conditions at 300 K. The temperature was maintained by using the Langevin thermostat, whereas the pressure was kept at 1 bar using the Berendsen barostat [40]. The time step was set to 2 fs. Long-range electrostatic interactions were treated using the Particle Mesh Ewald method [41] with a cut-off of 10 Å. Bond lengths involving hydrogen atoms were constrained by SHAKE [42]. Analyses of the trajectories were carried out with CPPTRAJ [43].